Bioresource Technology 403 (2024) 130896

Contents lists available at ScienceDirect

Bioresource Technology

journal homepage: www.elsevier.com/locate/biortech

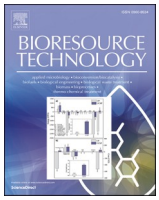

Comparing the performance of fluidized and fixed granular activated carbon beds as cathodes for microbial electrosynthesis of carboxylates from CO_2

Igor Vassilev, Johanna M. Rinta-Kanto, Marika Kokko *

Faculty of Engineering and Natural Sciences, Tampere University, Finland

HIGHLIGHTS

- Microbial electrosynthesis (MES) was employed to convert CO_2 to acetate.
- Fixed and fluidized granular activated carbon (GAC) biocathode beds were compared.
- Fixed GAC bed resulted in the highest acetate production rate of 204 ± 2 mg L^{-1} d^{-1}.
- Almost twice as high current density was obtained with fixed *vs.* fluidized GAC bed.
- Fluidized GAC bed was charged less efficiently than fixed GAC bed.

GRAPHICAL ABSTRACT

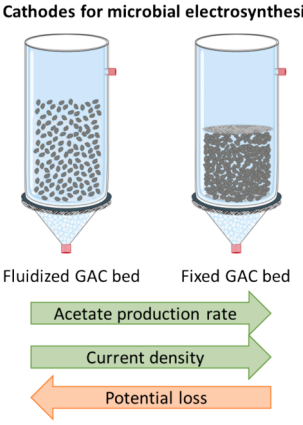

ARTICLE INFO

Keywords:
Cathode configuration
Bioelectrochemical system
Acetogenic mixed culture
Carbon capture and utilization

ABSTRACT

Microbial electrosynthesis (MES) can use renewable electricity to power microbial conversion of carbon dioxide (CO_2) into carboxylates. To ensure high productivities in MES, good mass transfer must be ensured, which could be accomplished with fluidization of granular activated carbon (GAC). In this study, fluidized and fixed GAC bed cathodes were compared. Acetate production rate and current density were 42 % and 47 % lower, respectively, in fluidized than fixed bed reactors. Although similar microbial consortium dominated by *Eubacterium* and *Proteiniphilum* was observed, lowest biomass quantity was measured with fixed GAC bed indicating higher specific acetate production rates compared to fluidized GAC bed. Furthermore, charge efficiency was the highest and charge recovery in carboxylates the lowest in fixed GAC beds indicating enhanced hydrogen evolution and need for enhancing CO_2 feeding to enable higher production rates of acetate. Overall, fixed GAC beds have higher efficiency for acetate production in MES than fluidized GAC beds.

* Corresponding author.
E-mail address: marika.kokko@tuni.fi (M. Kokko).

https://doi.org/10.1016/j.biortech.2024.130896
Received 14 February 2024; Received in revised form 22 May 2024; Accepted 23 May 2024
Available online 23 May 2024

1. Introduction

The fight against global warming requires the advancement of innovative technologies to produce carbon–neutral commodity chemicals and fuels from renewable feedstocks that are not fossil fuel-based and that do not compete with food production. Especially technologies such as microbial electrosynthesis (MES), which allow the conversion and storage of the greenhouse gas carbon dioxide (CO_2) into value-added products, have the potential to mitigate climate change (Dessì et al., 2021). In MES, acetogenic microorganisms are cultivated as biocatalysts under mild and environmentally friendly operation conditions for the synthesis of organic acids and alcohols using CO_2 as the sole carbon source. The reducing power is provided by the cathode and taken up by the microorganisms potentially directly in the form of electrons or hydrogen (H_2) produced via water electrolysis (Karthikeyan et al., 2019). Therefore, the performance of MES is determined to large extent by the interaction between microorganisms and the cathode, which makes the choice of cathode material and its configuration crucial (Vassilev et al., 2022).

Carbonaceous electrodes are rated among the most promising and commonly used cathodes in MES systems (Quejigo et al., 2019). For example, carbon felts, brushes, graphite rods and granules efficiently support microbe-electrode interaction due to great biocompatibility and high specific surface area, which provides a sufficient surface for microbial growth and adequate supply of reducing equivalents to the microorganisms (Quejigo et al., 2019). Such carbonaceous cathodes were operated in various configurations and different reactor designs (Bajracharya et al., 2022). However, large fraction of the MES research has been performed in H-cells offering a simple design that is advantageous for fundamental research but unsuitable for applied research and scale-up due to the high ohmic losses created by long-distance between anode and cathode, high energy demands, and inefficient CO_2 supply (Krieg et al., 2014). Therefore, to bring MES closer to industrial application it is essential to develop scalable reactor designs. Multi-chamber reactors with flat parallel-plates (Jourdin et al., 2016) or tubular structures (Ganigué et al., 2015) reduce the distance between anode and cathode while increasing the membrane-to-volume ratio, and have the potential to be scaled up in volume or numbered up in series or parallel stacks (Dessì et al., 2021; Enzmann et al., 2019).

In every scalable reactor it is essential to ensure a high ratio of electrode surface to reactor volume, which can be achieved with granular activated carbon (GAC) beds (Quejigo et al., 2019). However, densely packed GAC beds can face challenges such as mass transfer limitations, clogging and channels creating stagnant regions in the bed (Bajracharya et al., 2022). One solution could be fluidization of the bed, which can improve mixing of the bed and mass transfer between liquid medium (nutrients), gaseous substrates (CO_2, H_2), solid electrode (reducing power source) and biocatalysts (Borsje et al., 2021b; Quejigo et al., 2019). The benefits of a fluidized granular beds have been demonstrated in microbial fuel cells, where the microorganisms degrade organic matter from waste streams and use the granular bed anode as an electron acceptor for electrical power generation, while the fluidization of the anode bed has been reported to increase the current output (Borsje et al., 2021b, 2021a; Deeke et al., 2015; Kong et al., 2011). The use of fluidized GAC beds as cathodes was successfully demonstrated in tubular reactors were GAC bed was fluidized with medium recirculation with bacteria using the GAC bed as the electron donating cathode to reduce nitrate and produce H_2 (Sara et al., 2020). In other studies focusing on the cathode, GAC was fluidized through mixing via a magnetic stirrer in H-cells, where increased amount of GAC enhanced MES of acetate from CO_2 (Dong et al., 2018; Shakeel and Khan, 2022). However, in the MES studies with fluidized bed cathodes, the impact of fluidization of the bed on MES was not accurately evaluated. In fact, the studies compared a defined amount of fluidized GAC to a system either comprising only a current collector or to an increased amount of GAC (Dong et al., 2018; Shakeel and Khan, 2022). A comparison of MES performance with a fluidized and a fixed bed with the same amount of GAC and under comparable operation and cultivation conditions to evaluate the true benefits of fluidized beds over traditional fixed beds is still missing.

Therefore, in this study, a tubular BES was designed, which allowed the assay of a fixed and fluidized GAC bed cathode for MES. To investigate the effect of fluidization, the amount of GAC and operation parameters were fixed. MES performances with different GAC bed cathode configurations were evaluated through how efficiently CO_2 was converted into acetate and compared to MES performance of a BES without a GAC bed. In addition, the implications of fluidized cathodes on planktonic and biofilm growth, microbial community composition, and electrochemical GAC bed charging were studied.

2. Materials and methods

2.1. Mixed culture and cultivation medium

The original mixed culture was taken from a cow rumen provided by Natural Resources Institute Finland (Jokioinen, Finland). The culture was selectively enriched in a cathode chamber of flat-plate MES reactors comprising a graphite granular bed cathode (113 g EC-100 graphite granules; Graphite Sales, USA) by feeding the microorganisms with 100 % CO_2 and electricity as the sole carbon source and power source, respectively, in a fed-batch mode for more than one year. Effluent from the enrichment culture from the flat-plate reactors (200 mL) was used as inoculum for each tubular bed reactor.

800 mL minimal growth medium with a pH of ca. 7.2 was used in the cathode chamber and recirculation bottle of the tubular reactor consisting of 18 g L^{-1} Na_2HPO_4 $2H_2O$, 3 g L^{-1} KH_2PO_4, 3 g L^{-1} NH_4Cl, 15 mg L^{-1} $CaCl_2$, 20 mg L^{-1} $MgSO_4$ $7H_2O$, 2.1 mg L^{-1} sodium 2-bromoethanesulfonate, 1 g L^{-1} yeast extract as well as 10 mL L^{-1} trace elements solution (10 g L^{-1} EDTA, 1.5 g L^{-1} $FeCl_3$ $6H_2O$, 0.18 g L^{-1} KI, 0.15 g L^{-1} $CoCl_2$ $6H_2O$, 0.15 g L^{-1} H_3BO_3, 0.12 g L^{-1} $MnCl_2$ $4H_2O$, 0.12 g L^{-1} $ZnSO_4$ $7H_2O$, 0.06 g L^{-1} Na_2MoO_4 $7H_2O$, 0.03 g L^{-1} $CuSO_4$ $5H_2O$, 23 mg L^{-1} $NiCl_2$ $7H_2O$) and 1 mL/L vitamin solution (2.0 mg L^{-1} biotin, 2.0 mg L^{-1} folic acid, 10.0 mg L^{-1}pyridoxine-HCl, 5.0 mg L^{-1} thiamine-HCl, 5.0 mg L^{-1} riboflavin, 5.0 mg L^{-1} nicotinic acid, 5.0 mg L^{-1} D-Ca-pantothenate, 0.1 mg L^{-1} vitamin B12, 5.0 mg L^{-1}p-aminobenzoic acid, 5.0 mg L^{-1} lipoic acid). In the abiotic electrochemical control experiments, yeast extract and sodium 2-bromoethanesulfonate were omitted to minimize risk of medium contamination. The medium was sterilized by filtration (0.2 μm, Fisherbrand™ Disposable PES Filter Units, USA) and sparged with N_2 to remove dissolved oxygen from the medium.

2.2. Up-flow bioelectrochemical reactor setup

In this study, an up-flow glass reactor with a diameter of 4.7 cm, a height of 25.5 cm and an internal volume of 465 mL was used to evaluate the impact of GAC bed fluidization on MES (Fig. 1). The total internal volume included a 4 cm cone at the bottom of the up-flow reactor, which was filled with 6 mm glass beads to equally distribute the medium flow to the reactor. A polyester plastic mesh was installed above the glass bead bed with the help of o-ring and 3D-printed circular plastic support (see supplementary material) to avoid mixing of glass beads with the above GAC and to maintain the GAC in the up-flow reactor. A circular titanium mesh (ca. 4.7 cm diameter, 18 mesh woven from 0.28 mm diameter wire, Alfa Aesar, Germany) connected to a potentiostat (VMP3, BioLogic, France) via a titanium wire (length 11 cm, diameter 0.5 mm, 99.6+% purity, Goodfellow, Germany) was placed on top of the plastic mesh acting as the current collector. An Ag/AgCl reference electrode (+0.206 V vs. normal hydrogen electrode, BASi, USA) was inserted into the reactor through a glass port of the reactor in proximity to the current collector. The titanium mesh was covered by 34 g GAC (ca. 0.7 mm diameter, Cyclecarb 305, Chemviron Carbon, Belgium), which was previously washed in 100 %, 70 % and 30 % 2-propanol followed by

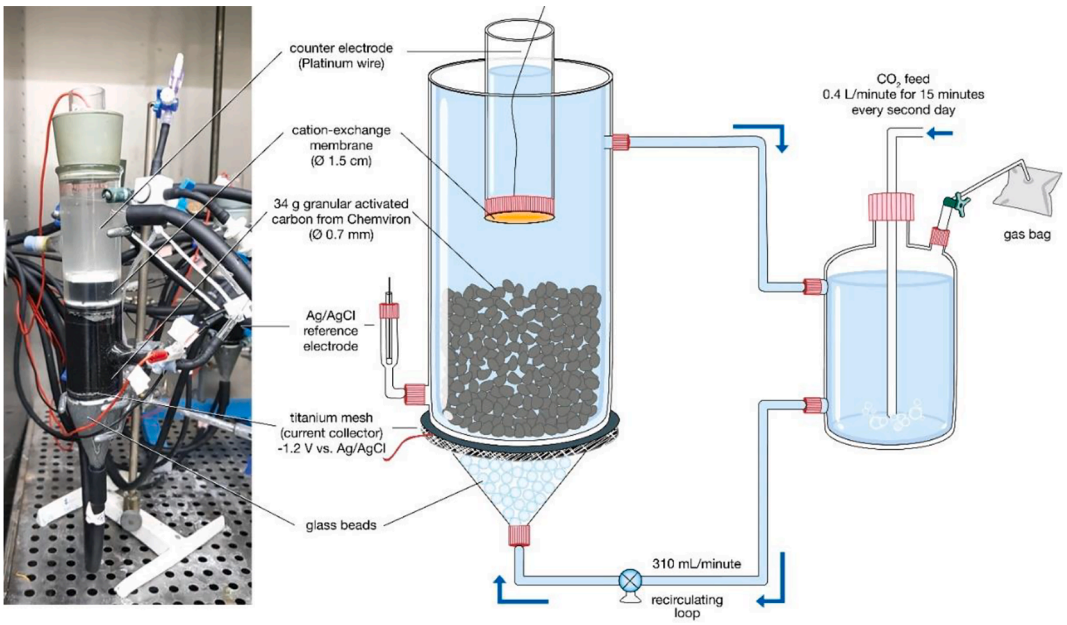

Fig. 1. The microbial electrosynthesis reactor utilised. In fluidized GAC bed reactors, the granules floated freely with the fluidization provided through recirculation of the growth medium. In fixed GAC bed reactors, the GAC bed was fixed by placing a plastic mesh on the stagnant GAC bed to keep it tightly packed.

distilled water for 30 min each. A second plastic mesh with an o-ring and a 3D-printed circular support was mounted above the GAC bed to prevent a GAC washout. In the fixed GAC bed, the mesh was in direct touch with the GAC bed keeping it tightly packed and preventing GAC movement, while in the fluidized GAC bed the mesh was positioned a few cm above the GAC bed enabling unhindered fluidization, and in the control reactor without GAC bed the mesh was omitted. The top of the up-flow reactor was sealed with a rubber stopper. A glass tube with a circular cation-exchange membrane (1.5 cm diameter, Membranes International, USA) at the bottom was installed in the upper part of the reactor through a hole in the rubber stopper. The glass tube assembled the anode chamber and contained 30 mL 50 mM H_2SO_4 and a platinum wire (15 cm length, 0.40 mm diameter, 99.95 % purity, Advent research materials, UK) as the anode. Close to the rubber stopper, a second glass port created the medium outlet, which was connected to a 0.5 L recirculation Schott bottle. The bottle was linked to a 5 L gas bag (Supel™-Inert Gas Sampling Bags, MERCK, Germany) and a CO_2 sparging tube reaching the bottom of the bottle.

2.3. Reactor operation and cultivation conditions

In all reactors, if not otherwise specified, the medium was recirculated with a velocity of 0.31 L min^{-1}, which resulted in a ca. 16 % height increase of the GAC bed in the fluidized bed reactor. At the beginning of each batch, the medium was sparged through the recirculation bottle for 30 min with 0.4 L CO_2 per min with a rotameter and a cathode potential of −1.2 V (all potentials herein are reported with respect to the Ag/AgCl reference electrode) was applied for at least 10 h to reach a stable current. To gain information on the role of the pure electrocatalyst (i.e., cathode) in the MES process, abiotic electrochemical control tests were performed with the different GAC bed configurations for 10 days at −1.2 V cathode potential. In the biological experiments, the reactor was inoculated with 200 mL enrichment culture and operated under the same conditions as the abiotic control test. The operating time of the biological experiments was dependent on time point when microbial acetate production stagnated, which varied between 36 and 64 days. In addition to fluidized, fixed and no GAC beds, a further bed configuration was evaluated, namely fixed bed, which was transformed into a fluidized bed after 16 days of operation. All experiments were performed in semi-batch mode at 35 °C, whereby the medium was supplied in batch mode and gaseous CO_2 was sparged to the recirculation bottle at 0.4 L min^{-1} for 10 min every other day. During the last 8 min of sparging the CO_2 was caught in the attached gas bag to ensure enriched CO_2 gas phase in the reactor headspace. All biological experiments were performed in duplicates.

To understand the impact of GAC bed fluidization on current output and bed charging further abiotic experiments were performed. The current was recorded at −1.2 V applied cathode potential at different medium recirculation velocities: 0 (no mixing), 0.11, 0.21 and 0.31 L min^{-1}. The bed charging efficiency was evaluated at 0.31 L min^{-1} medium recirculation measuring the potential of the top layer of the bed via a second three-electrode setup. More precisely, a second circular titanium mesh electrode was placed on top of the GAC bed with a second Ag/AgCl reference electrode next to it, while a second platinum wire was inserted in the anode chamber as the counter electrode. −1.2 V was only applied at the titanium mesh at the bottom of the bed, while the second titanium mesh was used to measure the open circuit potential at the top layer of the bed.

The mechanical stability of the GAC under fluidization was tested at a medium recirculation velocity of 0.31 L min^{-1} in the tubular reactor without integrated electrodes. After 15, 30 and 60 d of fluidization granules were sampled and their diameter was determined via a CCD high-speed camera (1380 × 1090 resolution, AVT Marlin 145-B2). At least 280 granules of each sampling time point were scattered on an illuminated glass plate and pictured. The method is described in detail in Tolvanen and Raiko (2014). The diameter was determined with an analysis program recognizing the granule projection outlines and calculating the pixel-based projection area (Honkanen et al., 2005).

2.4. Analyses and calculations

Every second day, 2.5 mL samples of liquid phase were taken from the catholyte recirculation bottles. Half of the sample was used to measure the pH (WTW-330i pH meter, Germany) and the optical density at 600 nm (OD_{600nm}) with a UV–Vis spectrophotometer (UV-1800, Shimadzu, Japan). The other half was immediately filtered through a 0.2 μm pore filter for quantitative analysis of volatile fatty acids (VFAs) and alcohols via gas chromatograph with a flame ionization detector (GC-FID 2010 Plus, Shimadzu, Japan), equipped with AOC-20 s autosampler and a Zebron ZB-WAX plus column (0.25 um diameter, 30 m

length). Helium was used as carrier gas and had a flow rate of 84.4 mL min^{-1}. The column was firstly programmed at 160 ℃, with a rise of 20 ℃ min^{-1}, and further increased to 220 ℃, with a rise of 40 ℃ min^{-1}, then held for 3 mins. The injector and detector temperatures were set at 250 ℃.

To determine the CO_2, H_2 and CH_4 content in the reactor, gas samples from the gas bag were analyzed via gas chromatograph with a thermal conductivity detector (GC-TCD 2014, Shimadzu, Japan) equipped with an Agilent J&W packed GC column (2.00 mm internal diameter, 1.8 m length). Nitrogen was used as the carrier gas with a flow rate of 20 mL min^{-1}. The temperature of the injector, column, and detector was set at 110 ℃, 80 ℃, and 110 ℃, respectively (Nissilä et al., 2011). The volume in the gas bag was measured via a water replacement method, in which the volume of the gas is equalized to the volume of the replaced water in the water pillar.

The percentage of electrons from the cathode recovered in organic carbon products is provided as charge efficiency (ε_C) calculated per *Eq. (1)*, where F is the Faraday's constant (96485.3365 C/mol), m_i is the absolute quantity of product i in mol at a specific time t (see Table S1), DOR the degree of reduction of the product i and $\int I\,dt$ is the integration of produced current over time t, which yields the overall charge transfer in the electrochemical system.

$$\varepsilon_C = \frac{F \times \sum_i (m_i \times DOR_i)_t}{\int I dt} \times 100 \quad (1)$$

The statistical analysis was carried out with a Student's *t*-test, where the differences were considered statistically significant when the p-value was below 0.05.

2.5. Characterization of the microbiome

The morphology of the biofilm grown on the GAC was studied via scanning electron microscopy (SEM). At the end of each batch, ca. 10 g of wet GAC and a small piece of the titanium mesh (current collector) were taken to study the morphology of the biofilm grown under different electrode configuration. The granules and the mesh were firstly gently washed with 0.1 mol L^{-1} phosphate buffer solution to remove planktonic cells and then fixed within 2.5 % glutaraldehyde (dissolved in PBS) for 24 h at 4 ℃. The samples were then washed with PBS and dehydrated in a graded series of ethanol (10 %, 30 %, 50 %, 70 %, 80 %, 90 %, 100 %) for 10 min each at 80 rpm shaking. 3–4 treated granules were fixed with carbon glue on an aluminum SEM stub. The mesh was cut into small pieces and fixed with carbon tape on the aluminum SEM stub. The fixed samples were carbon coated to avoid charging and destroying of biofilms during SEM imaging by an electron beam. Images were obtained by a scanning electron microscope (JSM-IT500, JEOL Ltd.) with an applied acceleration voltage of 15 kV and with a secondary electron detector to maximize topographic contrast.

The characterization of the mixed culture was done via 16 s rRNA amplicon sequencing from samples of planktonic cells and biofilm (*i.e.*, growing on the surface of GAC). At the end of each batch, planktonic cells were harvested by centrifuging 2 × 40 mL broth from the reactor (1000 × *g*, 7 min, 4 °C), and resuspending the pellet in 0.2 mL 0.1 mol L^{-1} sterile phosphate buffer (PBS), which was then used for DNA extraction. To obtain biofilm samples, 2 × 21 g of wet GAC were collected after each batch, immediately washed 3 times with sterile PBS to remove planktic cells, and ultrasonicated (40 % amplitude, Soniprep 150 Plus, UK) in 15 mL sterile PBS for 1 min. The liquid phase containing the dissolved cells from the biofilm was centrifuged (1000 × *g*, 7 min, 4 °C). Those steps were repeated 7 times with the same GAC samples to ensure gentle but efficient removal of biofilm from the GAC. The combined pellets were resuspended in 1 mL of sterile PBS, stored at −80 °C, and afterwards used for DNA extraction. The DNA was extracted using a DNeasy kit PowerSoil Pro Kit (Qiagen, Germany) following the manufacturer's protocol and the DNA was quantified with NanoDrop.

The abundance of bacteria in planktonic and biofilm samples was estimated via 16S rRNA gene copy quantification by quantitative polymerase chain reaction (qPCR) analysis with a Bio-Rad CFX96 (CFX96 Touch Real-Time PCR Detection System, Bio-Rad, USA). The qPCR method was adopted from (Rinta-Kanto et al., 2016). Briefly summarized, 25 μL qPCR reactions contained ultrapure water, 1× Maxima SYBR Green Master Mix (Thermo Fisher Scientific), 0.5 μM of primer Eub338 and Eub518 (which target the V3-V4 region of eubacterial 16S rRNA) (Fierer et al., 2005) and 5 μL of 100-times diluted DNA (sample, standard or ultrapure water lacking DNA as control). All qPCR reactions were run in triplicates with following program: denaturation at 95 ℃ for 10 min, 34 cycles of 95 ℃ for 15 s, and 62 ℃ for 1 min followed by a melting curve analysis.

The DNA samples were used for 16 s rRNA amplicon sequencing to study the microbial community composition. Preparation of amplicon libraries of 16S rRNA genes and sequencing took place commercially at Novogene (Cambridge, UK) with Illumina Novaseq 6000 system. Bioinformatics were carried out using Qiime 2, version 2021.4 (Bolyen et al., 2019). After quality filtering the amplicon data comprised 744,845 reads assigned in 401 amplicon sequence variants (ASVs) from 14 samples. Demultiplexed, trimmed and quality-filtered paired end sequences were joined and denoised, then assigned into ASVs with DADA2 (Callahan et al., 2016). The ASVs were aligned with MAFFT (Katoh et al., 2002) and used to construct a phylogeny with fasttree2 (Price et al., 2010). Taxonomic classification of the ASVs was completed using the q2-feature-classifier (Bokulich et al., 2018) against Greengenes 13_8 99 % OTUs full-length sequences (McDonald et al., 2012). The data obtained during this study was deposited at the European Nucleotide Archive under project accession number PRJEB75778.

3. Results

3.1. Fixed granular bed outperformed fluidized granular bed in microbial electrosynthesis

An up-flow reactor was characterised for MES of carboxylates with fluidized and fixed GAC beds and the performance was compared to up-flow reactor without GAC. Acetate was selectively produced (≥93 %) in all the cathode configurations, while butyrate concentrations remained below 0.74 g L^{-1} (Fig. 2). Similar acetate titers were obtained in all the cathode configurations, *i.e.*, 6.4 ± 0.4, 6.6 ± 0.5 and 6.2 ± 1.2 g L^{-1} with fixed GAC bed, fluidized GAC bed and control without GAC, respectively. Acetate production rate, on the other hand, was almost double as high with fixed GAC bed (204 ± 2 g L^{-1} d^{-1}) compared to fluidized GAC bed (119 ± 20 g L^{-1} d^{-1}) and control without GAC (117 ± 24 g L^{-1} d^{-1}) (Table 1), which is statistically significant ($p < 0.05$). In abiotic conditions, no carboxylates were produced (see supplementary material). The pH decreased during the reactor runs and dropped faster in fixed GAC bed (from ca. 6.6 to 5.8 in 30 days) than in the other two cathode configurations (*i.e.*, from *ca.* 6.6 to 5.8 in fluidized GAC bed in 50 days and from *ca.* 6.6 to 5.9 without GAC bed in 40 days; Fig. 2) likely due to the higher production rates of acetate. The conductivity in the cathodic media remained rather stable, between 13 and 18 mS cm^{-1}, throughout the run (see supplementary material).

The average current densities obtained at fixed cathode potential of −1.2 V were −35 ± 13, −18 ± 2.4 and −14 ± 4.7 mA cm^{-2} in fixed GAC bed, fluidized GAC bed and without GAC bed, respectively (see supplementary material). No H_2 evolution and only trace amounts of CO_2 (<1.3 %) were detected at the cathodes during the runs. Overall, the charge transfer was the highest with fixed GAC bed (160 ± 60 kC) followed by fluidized GAC bed (128 ± 1.0 kC) and control without GAC (84 ± 3.5 kC), from which the latter two show a statistical significance ($p < 0.05$). Charge recovery in carboxylates, however, was the highest (85 ± 20 %) in the control reactor without GAC followed by fluidized GAC bed (63 ± 4 %) and fixed GAC bed (61 ± 27 %) indicating that in the control reactor, the electrons provided were utilised the most efficiently to

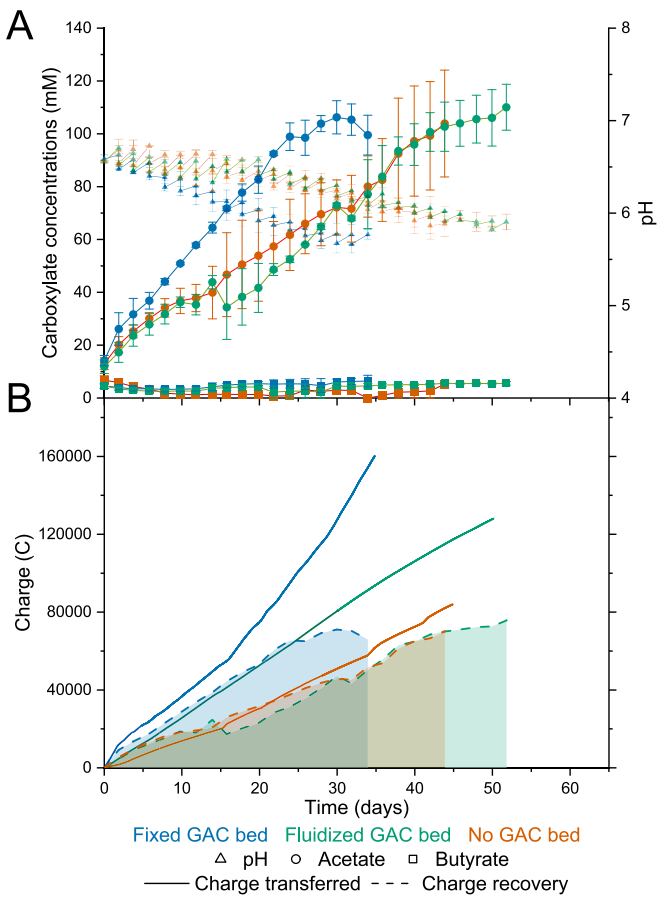

Fig. 2. Carboxylate, i.e., acetate and butyrate concentrations, and pH values (A) as well as charge transfer and charge recovery (B) in three different cathode configurations, including fixed GAC bed, fluidized GAC bed and without GAC bed. Standard deviations are given for duplicate runs.

Table 1
Acetate production rates, average current densities and coulombic efficiencies obtained with different granular activated carbon (GAC) bed cathode configurations.

		Acetate production rate (mg L^{-1} day^{-1})	Average current density (mA cm^{-2})	Coulombic efficiency (%)
Reactor with fixed GAC bed cathode		204 ± 2	35 ± 13	61 ± 27
Reactor with fluidized GAC bed cathode		119 ± 20	18 ± 2	63 ± 4
Reactor without GAC bed		117 ± 24	14 ± 5	85 ± 20
Reactor with GAC bed cathode changed from fixed to fluidized bed	Fixed GAC bed cathode	266 ± 60	52 ± 25	41 ± 22
	Fluidized GAC bed cathode	50 ± 10	12 ± 1	43 ± 14

Duplicate reactors were run for each condition.

produce carboxylates. However, as GAC can adsorb compounds, including carbohydrates, the actual charge recovery in carboxylates in fluidized and fixed GAC beds is likely higher than analysed as the GAC can adsorb also acetic acid. For example, abiotic adsorption experiments with a different GAC indicated that from 6.4 g L^{-1} acetate 68 % was adsorbed in 15 g GAC (results not shown).

Cathodic GAC beds have been studied as packed GAC beds (Brandão Lavender et al., 2022; Chatzipanagiotou et al., 2022; Liu et al., 2018; Mao et al., 2021; Shakeel and Khan, 2022) or fluidized beds where fluidisation is realized with magnetic stirrers (Dong et al., 2018; Kim et al., 2017; LaBarge et al., 2017; Ma et al., 2022) or with liquid recirculation (Sara et al., 2020), although only few of these studies concentrate on acetate production through MES. For example, increased acetate production rates and current densities of up to 140 mg L^{-1} d^{-1} and −0.4 A m^{-2}, respectively, were reported when the GAC addition was increased from 0 to 16 g L^{-1} GAC in H-type two-chamber MES that fluidized GAC beds by mixing with magnetic stirrer (Dong et al., 2018). However, the fluidized GAC bed was not compared to fixed GAC bed, so it is not clear whether fluidization of the GAC bed improved MES performance. Furthermore, utilizing H-type two-chamber MES with a combination of packed and fluidized GAC resulted in acetate production rates of 160 mg L^{-1} d^{-1} (Shakeel and Khan, 2022), while packed GAC beds were investigated in two-chamber MES with GAC with and without Ni doping resulting in the highest acetate yield of over 3 g L^{-1} with Ni doped GAC (Chatzipanagiotou et al., 2022). Thus, the acetate production rates and yields obtained in this study are in the same range previously reported with GAC biocathodes.

The energy consumption was lower without GAC (25 ± 7 kWh kg^{-1} acetate) than with fluidized GAC bed (48 ± 2 kWh kg^{-1}) and fixed GAC beds (68 ± 23 kWh kg^{-1}). Thus, integration of GAC to the cathodes increased the energy consumption, which, however, would likely be lower if the acetate presumably adsorbed in the GAC granules would be taken into account. Furthermore, the reactor configuration was not optimized in this study as the main purpose was to compare the performance of different cathode configurations and thus, the energy consumption could likely be decreased by paying more attention to the placement of the anode electrode as well as the surface area and placement of the membrane. Although low energy consumption of 2.07 kWh kg^{-1} acetate has been reported with thermophilic MES (Rovira-Alsina et al., 2022), ca. 50 kWh kg^{-1} was required to produce acetate in bubble column MES (Pan et al., 2023) and during a 300 day MES run the energy consumption increased from 10 to 18 to 200–250 kWh kg^{-1} acetate (Bajracharya et al., 2017).

3.2. *Effect of granular bed fluidisation on microbial electrosynthesis performance*

As mentioned above, no comparison between fixed and fluidized GAC beds has been reported before. Thus, the reasons for the superior performance of fixed against fluidized cathodic GAC beds for MES was further investigated. First, it was determined whether fixed GAC bed would enable faster growth of microorganisms that would enable higher acetate production rates also after converting fixed GAC bed to fluidized GAC bed. The reactor was started as fixed GAC bed and the conversion to fluidized GAC bed was done on day 16, when acetate and butyrate titers were 4.9 ± 1.5 g L^{-1} and 1.0 ± 0.5 g L^{-1}, respectively (Fig. 3). In the first 16 days with fixed GAC bed, the acetate production initiated immediately and reached acetate production rates of 226 ± 60 mg L^{-1} d^{-1}. After converting the GAC bed to fluidized mode, the acetate production became slower and in the following 34 days, the acetate titer only increased from 4.9 ± 1.5 to 5.9 ± 0.7 g L^{-1} (Fig. 3) with acetate production rate of 50 ± 10 mg L^{-1} d^{-1}. The current density was −52 ± 25 mA cm^{-2} in the first 16 days, after which it dropped to −12 ± 1.3 mA cm^{-2} indicating decreased performance of the fluidized GAC bed (see supplementary material). The charge efficiency in the periods of fixed and fluidized GAC bed were similar, 41 ± 22 % and 43 ± 14 %, respectively. The results indicate that the superior performance of the fixed GAC bed was not due to growth of microorganisms as the reactor performance deteriorated immediately after converting fixed GAC bed to fluidized GAC bed.

Second, the electrochemical performance of the fixed and fluidized GAC bed cathodes was determined in abiotic experiments by determining the effect of recirculation velocity on the current densities with GAC beds and potential gradient inside the GAC beds (Fig. 4). Increasing

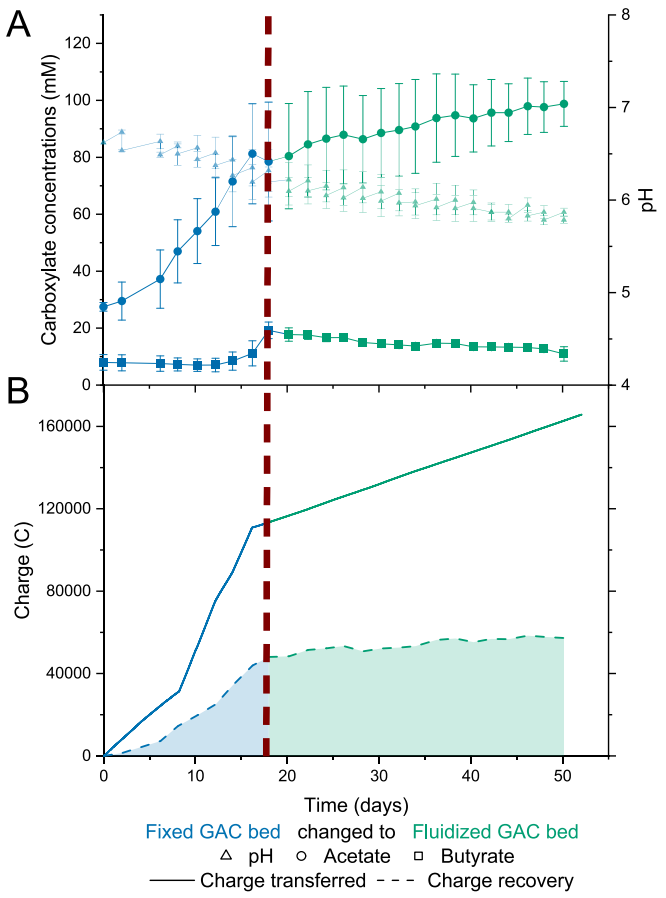

Fig. 3. Carboxylate, i.e., acetate and butyrate concentrations and pH values (A) as well as charge transfer and recovery (B) of reactors where fixed GAC bed cathode was converted to fluidized GAC bed on day 16. Standard deviations are given for duplicate runs.

recirculation velocity from 0 to 300 mL min^{-1} increased the current densities. However, the increase in current density was always at least double as high with fixed bed (increasing from -18 ± 1.3 mA cm^{-2} to -27 ± 3.8 mA cm^{-2}) compared to fluidized bed (increasing from -1.0 ± 0.1 mA cm^{-2} to -13 ± 0.6 mA cm^{-2}). The results are in line with the biological experiments where the average current density was almost double as high with fixed than fluidized GAC beds. Furthermore, it can be hypothesized that the recirculation velocity used in this study, i.e. 300 mL min^{-1}, is the optimal for carboxylate production and lower recirculation velocities would likely decrease acetate production. Although higher recirculation velocities were not studied, they may further enhance the current densities and acetate production.

Next, potential gradient across the fixed and fluidized GAC beds were determined. Fluidization of the bed resulted in high potential losses (624 ± 24 mV) in the upper layer of the GAC bed compared to the fixed GAC bed cathode (262 ± 20 mV), which was likely due to increased resistance, decreased contact between the granules, and decreased conductivity through the bed. Thus, fluidized GAC bed is likely less charged and can supply the bacteria less efficiently with reducing power resulting in slower acetate production rates. In contrast to the cathodic GAC bed studied here, with capacitive bioanodes approximately two-times higher current production has been reported with fluidized (moving bed where fluidization was created with gas lift and the GAC were recirculated through a discharge cell) than with fixed GAC bed (Borsje et al., 2021b). This was due to the capacitive currents that were increased with fluidized GAC bed due to long charging times and short discharging times of the moving bed (Borsje et al., 2021b). However, comparison of fixed and fluidized GAC beds at the biocathodes has not been reported before to

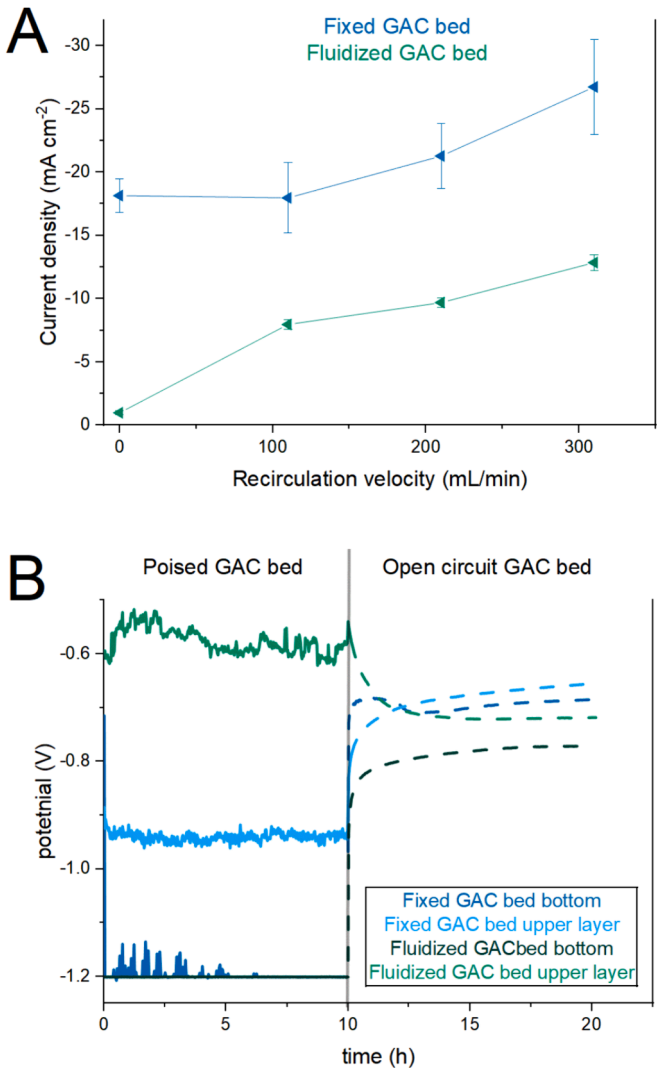

Fig. 4. Current densities at different recirculation velocities (A) and potential at the bottom and upper part (B) of fixed and fluidized GAC bed cathodes. Standard deviations are given for duplicate runs.

the author's knowledge. In this study, the potential loss through the fluidized GAC bed was the likely reason to decrease the acetate production rates and current densities.

The effect of fluidisation on GAC particles was also determined in abiotic runs by determining the diameters of the GAC every 15 days in a 60-day reactor run. The GAC disintegrated over time and the equivalent spherical diameter of the GAC decreased from 0.85 mm to 0.79, 0.73 and 0.70 mm from day 0 to days 15, 30 and 60, respectively, behaviour of which cannot be excluded during the biological MES runs (see supplementary material).

3.3. Biomass growth and microbial communities

The density of planktonic cells during the biological runs were monitored by measuring the OD_{600} of the recirculation liquid, while the number of cells were quantified with qPCR at the end of the reactor runs from the DNA extracted from biofilm and the recirculation liquid (Fig. 5). The highest OD_{600} was measured from the reactor without GAC followed by fluidized GAC bed and fixed GAC bed reactors. This is in accordance with the total 16 rRNA gene copies (absolute total in the reactor broth) as the highest number of gene copies in the planktonic samples were observed in the reactor without GAC bed followed by fluidized GAC bed and fixed GAC bed. In the reactors containing GAC,

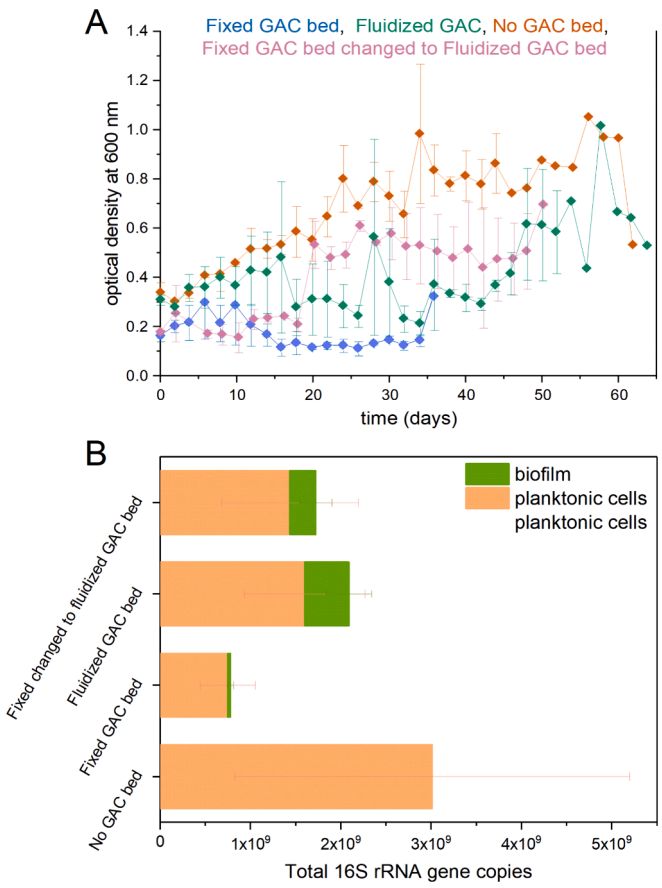

Fig. 5. Optical densities (A) and total 16S rRNA gene copies (B) measured from the different cathode configurations. The error bars present the duplicate reactors.

higher number of the total 16 rRNA gene copies in the biofilm was observed with fluidized than with fixed GAC bed. The lowest number of the total 16 rRNA gene copies were measured in fixed GAC bed, although it resulted in the highest carboxylate production rates, indicating superior performance of the cells towards carboxylate production, i.e. higher specific acetate production rates. SEM images indicate that cells prefer to grow in the pores of GAC, which may be partly due to the potential disintegration of the granules during the run (see supplementary material). SEM images also indicate that less cells grow on the GAC from the fixed bed cathode. Many cells were detected on the titanium mesh in the MES without GAC bed and with fixed GAC bed reactors, while not that many cells were observed on the titanium mesh from the fluidized GAC bed reactor. Furthermore, crystalline structures could be detected on the titanium mesh in the fluidized GAC bed and fixed GAC bed changed to fluidized bed reactors.

Eubacterium, *Proteiniphilum* and *Cellulosimicrobium* were the most abundant genera in the end of the reactor runs (Fig. 6). In the planktonic samples, the relative abundance of *Eubacterium* was the highest (38 ± 17 %) in MES without GAC, while in the fixed and fluidized GAC beds *Proteiniphilum* had the highest relative abundance (29 ± 25 % *vs.* 28 ± 8 %, respectively) followed by *Cellulosimicrobium* (29 ± 10 %) and *Eubacterium* (18 ± 1 %), respectively. In reactor where fixed GAC bed was converted to fluidized GAC bed, the relative abundance of *Cellulosimicrobium* was the highest (49 ± 9 %) in the planktonic samples. In the biofilm samples, *Eubacterium* was present at high relative abundance, *i.e.* 18 ± 1 %, 35 ± 25 % and 42 ± 7 % in fixed GAC bed, fluidized GAC bed and fixed GAC bed converted to fluidized GAC bed, respectively. In fixed and fluidized GAC beds, also *Proteiniphilum* had high relative abundance (25 ± 12 % and 26 ± 15 %, respectively), while fixed GAC bed also contained *Cellulosimicrobium* at higher relative abundance (15 ± 12 %). Overall, the total 16 rRNA gene copy numbers or microbial community results do not explain the differences in the MES performance between the different cathode configurations.

The cathodic microbial consortia contained *Eubacterium*, *Proteiniphilum* and *Cellulosimicrobium* as the most abundant genera. *Eubacterium limosum* has been utilized before in MES as part of an enrichment culture in biocathodes converting CO_2 to acetate and ethanol (Blasco-Gómez

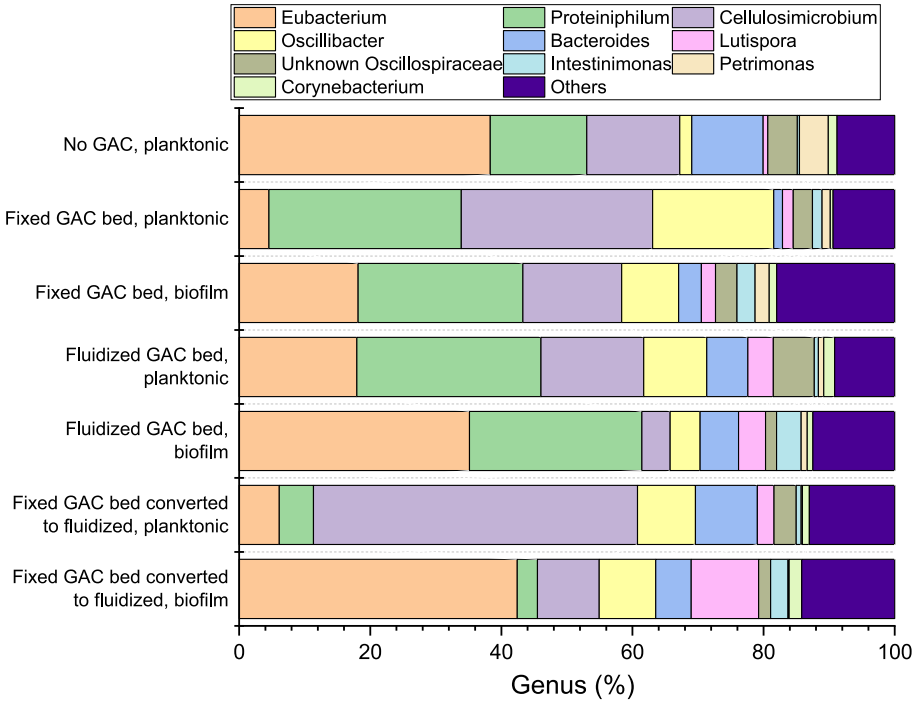

Fig. 6. Ten most abundant genera of the planktonic and biofilm samples collected at the end of the reactor runs with the different cathode configurations, including fixed GAC bed, fluidized GAC bed and without GAC bed. The results are given as means of two replicates.

et al., 2019; Romans-Casas et al., 2021). Members of *Proteiniphilum* have been detected in MES producing methane and they have been suggested to play a role in biological or bioelectrochemical H_2 evolution or act as a fermentative microbe (Cui et al., 2023; Flores-Rodriguez and Min, 2020). Both *Eubacterium* and *Proteiniphilum* were present at high abundance in the GAC biofilms, 18–42 % and up to 26 %, respectively, in this study indicating they likely had a role in conversion of CO_2 to acetate. The exact role of these species should be, however, further studied. *Cellulosimicrobium*, species of which have been reported to have cellulolytic properties (Bakalidou et al., 2002; Song and Wei, 2010), was more abundant in planktonic than in biofilm samples (at relative abundances of 14–49 % and 4–15 %, respectively). However, the exact role of *Cellulosimicrobium* in this study is not clear. Furthermore, it should be noted that the total 16 s rRNA amplicon sequencing only gives information on the species that are present in the microbial communities, not on the active species.

3.4. Implications and outlook

The highest acetate production rate achieved in this study was 0.20 ± 0.002 g L^{-1} d^{-1}. The highest acetate production rates reported in the literature range from 9.85 to 77 g L^{-1} d^{-1} and have been achieved with three dimensional electrodes, such as carbon felt and reticulated vitreous carbon (Jourdin et al., 2018, 2016, 2015; LaBelle and May, 2017). However, majority of the acetate production rates in MES have remained below 0.7 g L^{-1} d^{-1} (for a review, see *e.g.,* (Lee et al., 2021)). In this study, the focus was on comparison of different cathode configurations and thus, the reactor performance was not optimised. As no H_2 was observed and CO_2 content remained low (<1.3 %) in the cathodic gas bags in this study, H_2 and CO_2 were efficiently utilized for carboxylate production and the availability of electrons/H_2 and/or CO_2 were hindering the production rates of carboxylates. While continuous CO_2 feeding (Jourdin et al., 2019) and increasing availability of electrons (LaBelle and May, 2017) have improved the carboxylate production, also the increase of biomass has been reported to result in enhanced carboxylate production rates (Jourdin et al., 2018; LaBelle and May, 2017). Furthermore, the optimization of the current collector, as discussed below, will likely improve the MES performance. Thus, there are various ways of further optimizing the acetate production rates of the microbial culture and reactor set-ups used in this study.

In this study, the size and placement of the current collector were not optimized, and thus, it is crucial to further improve the contact between the GAC and current collector to decrease the contact resistance in the fluidized GAC beds. Similar approach on optimising the current collector has been suggested at fluidized anodes, where different reactor configurations have been evaluated. For example, the first fluidized bed reactors operated with relatively small discharge cell that did not have efficient contact between the granules and the discharge cell, i.e., current collector (Deeke et al., 2015) and thus, different approaches were determined. For example, placing two current collectors instead of one in the discharge cell and increasing the contact time between the GAC and the current collector enhanced the bioanode performance (Borsje et al., 2021a). However, it should be noted that the anodic GAC beds have a different working principle than biocathodes, where the GAC is charged upon microbial oxidation of organics in the wastewater and the current is released when the GAC are in contact with the current collector. In cathodic GAC beds, on the other hand, utilizing the capacitive properties of GAC has not been often reported and potential or current is often constantly applied and thus, the GAC is rather used to increase the surface area for biofilm growth. However, methane production in GAC biocathodes was enhanced at intermittent current mode, where higher methane production rates were reported when current was provided for the biocathode for longer periods (4 min on – 2 min off) (Liu et al., 2018), although it remained unclear to what extent electrons were stored in the GAC. Furthermore, when fluidizing the GAC beds, the characteristics of the GAC have to be carefully considered. For example, in this study the average diameter of granules decreased in abiotic fluidization experiment from 0.85 mm to 0.73 mm in 30 days. Thus, the slow degradation of the granules upon fluidization may negatively affect the biofilm formation.

4. Conclusions

In MES, fixed GAC bed cathodes resulted in the highest acetate production rates and current densities of 204 ± 2 mg L^{-1} d^{-1} and 34 ± 13 mA cm^{-2}, respectively, that were 71 % and 94 % higher compared to fluidized GAC bed cathode. Fixed GAC bed had higher charge efficiency and the lower biomass amount in fixed GAC bed accompanied with higher acetate production rates indicate higher specific acetate production rates. Acetate was selectively produced with similar titers of 6.2–6.6 g L^{-1} in all the reactors. Overall, fixed GAC beds showed superior performance for acetate production in MES when compared to fluidized GAC beds.

CRediT authorship contribution statement

Igor Vassilev: Writing – original draft, Visualization, Methodology, Investigation, Formal analysis, Conceptualization. **Johanna M. Rinta-Kanto:** Writing – review & editing, Investigation. **Marika Kokko:** Writing – review & editing, Supervision, Funding acquisition, Conceptualization.

Declaration of competing interest

The authors declare that they have no known competing financial interests or personal relationships that could have appeared to influence the work reported in this paper.

Data availability

Data will be made available on request.

Acknowledgements

The authors acknowledge the funding from Research Council of Finland (grant numbers 316657, 319910, and 346046). Special thanks go to Helena Vassilev for her support in designing Fig. 1. We would like to thank Henrik Tolvanen for his support in determining the diameter of the granules. We would like to acknowledge Tampere Microscopy Center facilities at Tampere University for taking the scanning electron microscopy images.

Appendix A. Supplementary data

Supplementary data to this article can be found online at https://doi.org/10.1016/j.biortech.2024.130896.

References

Bajracharya, S., Yuliasni, R., Vanbroekhoven, K., Buisman, C.J.N., Strik, D.P.B.T.B., Pant, D., 2017. Long-term operation of microbial electrosynthesis cell reducing CO_2 to multi-carbon chemicals with a mixed culture avoiding methanogenesis. Bioelectrochem. 113, 26–34.

Bajracharya, S., Krige, A., Matsakas, L., Rova, U., Christakopoulos, P., 2022. Advances in cathode designs and reactor configurations of microbial electrosynthesis systems to facilitate gas electro-fermentation. Biores. Technol. 354, 127178.

Bakalidou, A., Kämpfer, P., Berchtold, M., Kuhnigk, T., Wenzel, M., König, H., 2002. *Cellulosimicrobium variabile* sp. nov., a cellulolytic bacterium from the hindgut of the termite *Mastotermes darwiniensis*. Int. J. Syst. Evol. Microbiol. 52, 1185–1192.

Blasco-Gómez, R., Ramió-Pujol, S., Bañeras, L., Colprim, J., Balaguera, M.D., Puig, S., 2019. Unravelling the factors that influence the bio-electrorecycling of carbon dioxide towards biofuels. Green Chem. 21, 684–691.

Bokulich, N.A., Kaehler, B.D., Rideout, J.R., Dillon, M., Bolyen, E., Knight, R., Huttley, G. A., Gregory Caporaso, J., 2018. Optimizing taxonomic classification of marker-gene amplicon sequences with QIIME 2's q2-feature-classifier plugin. Microbiome 6, 90.

Bolyen, E., Rideout, J.R., Dillon, M.R., Bokulich, N.A., Abnet, C.C., Al-Ghalith, G.A., Alexander, H., Alm, E.J., Arumugam, M., Asnicar, F., Bai, Y., Bisanz, J.E., Bittinger, K., Brejnrod, A., Brislawn, C.J., Brown, C.T., Callahan, B.J., Caraballo-Rodríguez, A.M., Chase, J., Cope, E.K., Da Silva, R., Diener, C., Dorrestein, P.C., Douglas, G.M., Durall, D.M., Duvallet, C., Edwardson, C.F., Ernst, M., Estaki, M., Fouquier, J., Gauglitz, J.M., Gibbons, S.M., Gibson, D.L., Gonzalez, A., Gorlick, K., Guo, J., Hillmann, B., Holmes, S., Holste, H., Huttenhower, C., Huttley, G.A., Janssen, S., Jarmusch, A.K., Jiang, L., Kaehler, B.D., Kang, K.B., Keefe, C.R., Keim, P., Kelley, S.T., Knights, D., Koester, I., Kosciolek, T., Kreps, J., Langille, M.G.I., Lee, J., Ley, R., Liu, Y.-X., Loftfield, E., Lozupone, C., Maher, M., Marotz, C., Martin, B.D., McDonald, D., McIver, L.J., Melnik, A.V., Metcalf, J.L., Morgan, S.C., Morton, J.T., Naimey, A.T., Navas-Molina, J.A., Nothias, L.F., Orchanian, S.B., Pearson, T., Peoples, S.L., Petras, D., Preuss, M.L., Pruesse, E., Rasmussen, L.B., Rivers, A., Robeson, M.S., Rosenthal, P., Segata, N., Shaffer, M., Shiffer, A., Sinha, R., Song, S.J., Spear, J.R., Swafford, A.D., Thompson, L.R., Torres, P.J., Trinh, P., Tripathi, A., Turnbaugh, P.J., Ul-Hasan, S., van der Hooft, J.J.J., Vargas, F., Vázquez-Baeza, Y., Vogtmann, E., von Hippel, M., Walters, W., Wan, Y., Wang, M., Warren, J., Weber, K. C., Williamson, C.H.D., Willis, A.D., Xu, Z.Z., Zaneveld, J.R., Zhang, Y., Zhu, Q., Knight, R., Caporaso, J.G., 2019. Reproducible, interactive, scalable and extensible microbiome data science using QIIME 2. Nature Biotechnol. 37, 852–857.

Borsje, C., Sleutels, T., Buisman, C.J.N., Ter Heijne, A., 2021a. Improving the discharge of capacitive granules in a moving bed reactor. J. Environ. Chem. Eng. 9, 105556.

Borsje, C., Sleutels, T., Zhang, W., Feng, W., Buisman, C.J.N., ter Heijne, A., 2021b. Making the best use of capacitive current: Comparison between fixed and moving granular bioanodes. J. Power Sources 489, 229453.

Brandão Lavender, M., Pang, S., Liu, D., Jourdin, L., ter Heijne, A., 2022. Reduced overpotential of methane-producing biocathodes: Effect of current and electrode storage capacity. Biores. Technol. 347, 126650.

Callahan, B.J., McMurdie, P.J., Rosen, M.J., Han, A.W., Johnson, A.J.A., Holmes, S.P., 2016. DADA2: High-resolution sample inference from Illumina amplicon data. Nature Methods 13, 581–583.

Chatzipanagiotou, K.-R., Jourdin, L., Bitter, J.H., Strik, D.P.B.T.B., 2022. Concentration-dependent effects of nickel doping on activated carbon biocathodes. Catal. Sci. Technol. 12, 2500–2518.

Cui, K., Guo, K., Carvajal-Arroyo, J.M., Arends, J., Rabaey, K., 2023. An electrolytic bubble column with an external hollow fiber membrane gas–liquid contactor for effective microbial electrosynthesis of acetate from CO_2. Chem. Eng. J. 471, 144296.

Deeke, A., Sleutels, T.H.J.A., Donkers, T.F.W., Hamelers, H.V.M., Buisman, C.J.N., Ter Heijne, A., 2015. Fluidized capacitive bioanode as a novel reactor concept for the microbial fuel cell. Environ. Sci. Technol. 49, 1929–1935.

Dessì, P., Rovira-Alsina, L., Sánchez, C., Dinesh, G.K., Tong, W., Chatterjee, P., Tedesco, M., Farràs, P., Hamelers, H.M.V., Puig, S., 2021. Microbial electrosynthesis: Towards sustainable biorefineries for production of green chemicals from CO_2 emissions. Biotechnol. Adv. 46, 107675.

Dong, Z., Wang, H., Tian, S., Yang, Y., Yuan, H., Huang, Q., Song, Shun, T., Xie, J., 2018. Fluidized granular activated carbon electrode for efficient microbial electrosynthesis of acetate from carbon dioxide. Biores. Technol. 269, 203–209.

Enzmann, F., Stöckl, M., Zeng, A.P., Holtmann, D., 2019. Same but different–Scale up and numbering up in electrobiotechnology and photobiotechnology. Eng. Life Sci. 19, 121.

Fierer, N., Jackson, J.A., Vilgalys, R., Jackson, R.B., 2005. Assessment of soil microbial community structure by use of taxon-specific quantitative PCR assays. Appl. Environ. Microbiol. 71, 4117–4120.

Flores-Rodriguez, C., Min, B., 2020. Enrichment of specific microbial communities by optimum applied voltages for enhanced methane production by microbial electrosynthesis in anaerobic digestion. Biores. Technol. 300, 122624.

Ganigué, R., Puig, S., Batlle-Vilanova, P., Balaguer, M.D., Colprim, J., 2015. Microbial electrosynthesis of butyrate from carbon dioxide. Chem. Commun. 51, 3235–3238.

Honkanen, M., Saarenrinne, P., Stoor, T., Niinimäki, J., 2005. Recognition of highly overlapping ellipse-like bubble images. Measurem. Sci. Technol. 16, 1760–1770.

Jourdin, L., Grieger, T., Monetti, J., Flexer, V., Freguia, S., Lu, Y., Chen, J., Romano, M., Wallace, G.G., Keller, J., 2015. High acetic acid production rate obtained by microbial electrosynthesis from carbon dioxide. Environ. Sci. Technol. 49, 13566–13574.

Jourdin, L., Freguia, S., Flexer, V., Keller, J., 2016. Bringing high-rate, CO_2-based microbial electrosynthesis closer to practical implementation through improved electrode design and operating conditions. Environ. Sci. Technol. 50, 1982–1989.

Jourdin, L., Raes, S.M.T., Buisman, C.J.N., Strik, D.P.B.T.B., 2018. Critical biofilm growth throughout unmodified carbon felts allows continuous bioelectrochemical chain elongation from CO_2 up to caproate at high current density. Frontiers Energy Res. 6, 7.

Jourdin, L., Winkelhorst, M., Rawls, B., Buisman, C.J.N., Strik, D.P.B.T.B., 2019. Enhanced selectivity to butyrate and caproate above acetate in continuous bioelectrochemical chain elongation from CO_2: Steering with CO_2 loading rate and hydraulic retention time. Biores. Technol. Reports 7, 100284.

Karthikeyan, R., Singh, R., Bose, A., 2019. Microbial electron uptake in microbial electrosynthesis: a mini-review. J. Ind. Microbiol. Biotechnol. 46, 1419–1426.

Katoh, K., Misawa, K., Kuma, K., Miyata, T., 2002. MAFFT: a novel method for rapid multiple sequence alignment based on fast Fourier transform. Nucleic Acids Res. 30, 3059–3066.

Kim, K.-R., Kang, J., Chae, K.-J., 2017. Improvement in methanogenesis by incorporating transition metal nanoparticles and granular activated carbon composites in microbial electrolysis cells. Int. J. Hydr. Energy 42, 27623–27629.

Kong, W., Guo, Q., Wang, X., Yue, X., 2011. Electricity generation from wastewater using an anaerobic fluidized bed microbial fuel cell. Ind. Eng. Chem. Res. 50, 12225–12232.

Krieg, T., Sydow, A., Schröder, U., Schrader, J., Holtmann, D., 2014. Reactor concepts for bioelectrochemical syntheses and energy conversion. Trends Biotechnol. 32, 645–655.

LaBarge, N., Yilmazel, Y.D., Hong, P.-Y., Logan, B.E., 2017. Effect of pre-acclimation of granular activated carbon on microbial electrolysis cell startup and performance. Bioelectrochem. 113, 20–25.

LaBelle, E.V., May, H.D., 2017. Energy efficiency and productivity enhancement of microbial electrosynthesis of acetate. Frontiers Microbiol. 8, 756.

Lee, S.Y., Oh, Y.-K., Lee, S., Fitriana, H.N., Moon, M., Kim, M.-S., Lee, J., Min, K., Park, G. W., Lee, J.-P., Lee, J.-S., 2021. Recent developments and key barriers to microbial CO_2 electrobiorefinery. Biores. Technol. 320, 124350.

Liu, D., Roca-Puigros, M., Geppert, F., Caizán-Juanarena, L., Na Ayudthaya, S.P., Buisman, C., ter Heijne, A., 2018. Granular carbon-based electrodes as cathodes in methane-producing bioelectrochemical systems. Frontiers Bioeng. Biotechnol. 6, 78.

Ma, J., Wang, Z., Li, L., Shi, Z., Ke, S., He, Q., 2022. Granular activated carbon stimulated caproate production through chain elongation in fluidized cathode electro-fermentation systems. J. Cleaner Prod. 365, 132757.

Mao, Z., Cheng, S., Sun, Y., Lin, Z., Li, L., Yu, Z., 2021. Enhancing stability and resilience of electromethanogenesis system by acclimating biocathode with intermittent step-up voltage. Biores. Technol. 337, 125376.

McDonald, D., Price, M.N., Goodrich, J., Nawrocki, E.P., DeSantis, T.Z., Probst, A., Andersen, G.L., Knight, R., Hugenholtz, P., 2012. An improved Greengenes taxonomy with explicit ranks for ecological and evolutionary analyses of bacteria and archaea. The ISME Journal 6, 610–618.

Nissilä, M.E., Tähti, H.P., Rintala, J.A., Puhakka, J.A., 2011. Effects of heat treatment on hydrogen production potential and microbial community of thermophilic compost enrichment cultures. Biores. Technol. 102, 4501–4506.

Pan, Z., Hu, X., Cai, W., Cui, K., Wang, Y., Guo, K., 2023. An electrolytic bubble column with gas recirculation for high-rate microbial electrosynthesis of acetate from CO_2. Ind. Eng. Chem. Res. 62, 16616–16621.

Price, M.N., Dehal, P.S., Arkin, A.P., 2010. FastTree 2 – Approximately maximum-likelihood trees for large alignments. PLoS ONE 5, e9490.

Quejigo, J.R., Tejedor-Sanz, S., Esteve-Núñez, A., Harnisch, F., 2019. Bed electrodes in microbial electrochemistry: setup, operation and characterization. ChemTexts 5, 4.

Rinta-Kanto, J.M., Sinkko, H., Rajala, T., Al-Soud, W.A., Sørensen, S.J., Tamminen, M.V., Timonen, S., 2016. Natural decay process affects the abundance and community structure of Bacteria and Archaea in *Picea abies* logs. FEMS Microbiol. Ecol. 92, fiw087.

Romans-Casas, M., Blasco-Gómez, R., Colprim, J., Balaguer, M.D., Puig, S., 2021. Bio-electro CO_2 recycling platform based on two separated steps. J. Environ. Chem. Eng. 9, 105909.

Rovira-Alsina, L., Dolors Balaguer, M., Puig, S., 2022. Transition roadmap for thermophilic carbon dioxide microbial electrosynthesis: Testing with real exhaust gases and operational control for a scalable design. Biores. Technol. 365, 128161.

Sara, T.S., Patricia, F.L., Carlos, M., Abraham, E.N., 2020. Fluidized bed cathodes as suitable electron donors for bacteria to remove nitrogen and produce biohydrogen. Electrochem. Commun. 116, 106759.

Shakeel, S., Khan, M.Z., 2022. Enhanced production and utilization of biosynthesized acetate using a packed-fluidized bed cathode-based MES system. J. Environ. Chem. Eng. 10, 108067.

Song, J.-M., Wei, D.-Z., 2010. Production and characterization of cellulases and xylanases of *Cellulosimicrobium cellulans* grown in pretreated and extracted bagasse and minimal nutrient medium M9. Biomass Bioenergy 34, 1930–1934.

Tolvanen, H., Raiko, R., 2014. An experimental study and numerical modeling of combusting two coal chars in a drop-tube reactor: A comparison between N_2/O_2, CO_2/O_2, and $N_2/CO_2/O_2$ atmospheres. Fuel 124, 190–201.

Vassilev, I., Dessì, P., Puig, S., Kokko, M., 2022. Cathodic biofilms – A prerequisite for microbial electrosynthesis. Biores. Technol. 348, 126788.